9950-1146

(NASA-CR-176101) DEVELOPMENT OF HIGH-EFFICIENCY SOLAR CELLS ON SILICON WEB (Westinghouse Research and) 25 p HC A02/MF A01 CSCL 10B

N85-33568

Unclas G3/44 25778

DIST. CATEGORY UC-63
DOE/JPL-956786/85/4
DRD NO. SE5
DRL NO. 211

DEVELOPMENT OF HIGH-EFFICIENCY SOLAR CELLS ON SILICON WEB

A. Rohatgi, D. L. Meier, R. B. Campbell
T. W. O'Keeffe, and P. Rai-Choudhury

Fourth Quarterly Progress Report
January to March 1985

This work was performed for the
Jet Propulsion Laboratory

Contract No. 956786

April 1, 1985

This report was prepared for the Jet Propulsion Laboratory, California Institute of Technology, sponsored by the National Aeronautics and Space Administration.

Westinghouse R&D Center
1310 Beulah Road
Pittsburgh, Pennsylvania 15235

This report was prepared as an account of work sponsored by the United States Government. Neither the United States nor the United States Department of Energy, nor any of their employees, nor any of their contractors, subcontractors, or their employees, makes any warranty, expressed or implied, or assumes any legal liability or responsibility for the accuracy, completeness or usefulness of any information, apparatus, product or process disclosed, or represents that its use would not infringe privately owned rights.

CONTENTS

LIST OF FIGURES..... iii

LIST OF TABLES..... iii

1. SUMMARY..... 1

2. INTRODUCTION..... 3

3. TECHNICAL PROGRESS..... 5

3.1 Approach to Polysilicon Emitter Solar Cells..... 5

3.2 Results On Cells With Polysilicon/Ti-Pd-Ag Grid..... 6

3.3 Resistivity and Lifetime Considerations For High-Efficiency Web Cells..... 13

4. PROGRAM STATUS..... 17

4.1 Present Status..... 17

4.2 Future Activity..... 17

5. REFERENCES..... 19

6. ACKNOWLEDGEMENTS..... 20

LIST OF FIGURES

Figure 1	Polysilicon emitter/grid designs for high-efficiency solar cells	7
Figure 2	Spreading resistance profiles for: a) 2800 Å polysilicon deposition followed by 950°C $POCl_3$ diffusion; b) 6-3/4 ion milling after $POCl_3$ diffusion; c) ion milling followed by 800°C/15 minutes N_2/5 minute O_2 heat treatment	9
Figure 3	Optical photograph of polysilicon grid lines defined by ion milling	10
Figure 4	Reflection high-energy diffraction (Rheed) pattern of the: a) silicon surface after 6-3/4 minute argon ion milling and b) ion-milled surface after 800°C/15 minute N_2/5 minute O_2 heat treatment	11

LIST OF TABLES

Table 1	SPV Diffusion Length Measurements After 6.75 min Ion Milling and Ion Milling Followed By 800°C/15 min N_2/5 min O_2 Heat Treatment	12
Table 2	A Comparison of the Lighted I-V Data	13
Table 3	Model Calculations For Resistivity and Diffusion Length Requirements For 17.5% Efficient Web Solar Cells	14
Table 4	Milestone Chart	18

PRECEDING PAGE BLANK NOT FILMED

1. SUMMARY

This monthly report discusses a novel approach to high-efficiency silicon solar cells in which the cell designs consist of doped polysilicon regions in the emitter and/or in the grid regions of the solar cells. These designs should work more effectively for cells in which V_{oc} is limited by emitter recombination. The n^+ polysilicon emitter is believed to lower hole mobility and bandgap narrowing compared to a single-crystal silicon emitter, thus reducing the emitter contribution to the reverse saturation current and giving higher V_{oc}.

Polysilicon/metal grid contacts can be used effectively to reduce recombination at the conventional metal grid contacts. In order for the above condition to be satisfied, the minority carrier diffusion length, L_p, in the polysilicon should be much less than the poly thickness ($L_p < W$). The polysilicon spacer under the metal grid should reduce the recombination velocity at the grid/emitter interface and give higher V_{oc}. This could actually produce results equivalent to an MIS contact with the advantage that the polysilicon technology is much more controlled and reproducible than a thin tunneling oxide.

Polysilicon deposition and $POCl_3$ diffusion conditions have been developed for poly emitter solar cells, and solar cells have actually been fabricated according to one of the designs. In these cells, polysilicon grid lines were defined by ion-milling and polysilicon was removed from the remainder of the emitter. Preliminary results indicate that the heat treatment subsequent to ion-milling resulted in a loss of carrier lifetime, partly because of a lower than expected V_{oc}. In the first run, V_{oc} of the cells was at most equal to that of the conventional cells, where no poly deposition was performed and the dopant surface concentration on the emitter was $2 \times 10^{20} cm^{-3}$. More

experiments are in progress to preserve carrier lifetime and optimize the polysilicon emitter design for high-efficiency cells.

Model calculations were also done in this period to determine the resistivity and diffusion length requirements for achieving 17-18% efficient web cells. Calculations indicate that a combination of front- and back-surface passivation and double-layer AR coating will give 17.5% efficient cells on 4 ohm-cm, 150 μm thick web crystals only when the minority carrier diffusion length becomes 467 μm. However, a diffusion length of only 125 μm will be required to achieve 17.5% efficient web cells if the bulk resistivity is dropped from 4 ohm-cm to 0.2 ohm-cm. These calculations do not account for any losses that may occur due to twin plane activity.

2. INTRODUCTION

The idealized efficiency of a silicon solar cell is about 25%, assuming the best material and surface parameters achievable to date, although present day cells fall considerably short of this limiting value. This is largely a consequence of heavy doping effects, bandgap narrowing, and high recombination at and near the cell surfaces. The major problems of efficiency improvement fall in the above categories; however, additional design requirements are essential for efficient contacts and antireflective coating. Although these areas are well understood, they are not insignificant and must be optimized consistent with device structure.

Starting material is equally important for high-efficiency cells because device fabrication and design are academic if the starting material quality is poor or it degrades rapidly with processing. The objective of this program is to understand and improve web silicon so that high-efficiency web cells can be fabricated using advanced cell design and processing.

It is clear that high efficiency is a major attribute that will enhance the large-scale applicability of photovoltaic systems. Systems calculations indicate that for very large-scale terrestrial applications, > 15% efficient photovoltaic modules will be required at a cost of ~50 cents/watt. This implies that ~18% efficient cells will be needed at low cost. Dendritic web silicon is a single-crystal silicon ribbon that has great potential for low-cost and high-efficiency solar cells. In this program we are trying to understand the loss mechanisms in dendritic web silicon by investigating the electrical activity of twin planes, the role of impurities and defects in web, impurity interaction with twin planes, starting web material quality, and the

effect of heat treatment and gettering on web quality. An improved understanding of the above effects should lead to fabrication of ~18% efficient web cells with good uniformity. This fourth quarterly report describes progress toward the development of high-efficiency solar cells on web silicon. Reported here is a novel approach to the high-efficiency cell using polysilicon in the emitter region and under the metal grid. Model calculations for resistivity and lifetime considerations for high-efficiency web cells are also shown.

3. TECHNICAL PROGRESS

3.1 Approach to Polysilicon Emitter Solar Cells

This report describes a novel approach to high-efficiency cells which consists of using heavily doped polysilicon in the emitter region of the solar cells. Doped polysilicon emitters have been successfully used in integrated circuits to increase the emitter injection efficiency and the common emitter gain (β) of the bipolar transistors.[1-5] Some investigators believe that either: a) an interfacial oxide layer between the silicon and polysilicon provides a barrier for hole transport through the emitter, b) heavily doped polysilicon has smaller amounts of bandgap narrowing, or c) hole mobility in the polysilicon is much smaller than in the crystalline silicon. All three models lead to a reduction in hole saturation current density, J_{po} or J_{oe}, in the emitter and, therefore, reduced base current ($J_p = J_{po} \exp qV_{EB}/kT$) and higher common emitter gain ($\beta = \frac{I_c}{I_b}$):

$$J_{po} = \frac{q\, D_p}{N_D} \cdot \frac{(n_i\, e^{\Delta V_G/V_T})^2}{W_E} \quad \text{for } L_p > W_E$$

Thus, lower hole mobility or a smaller value of D_p and smaller bandgap narrowing (ΔV_G) in polysilicon will reduce J_{po}. The ratio of the emitter Gummel number with and without the polysilicon is given by

$$k \equiv \frac{G_e\,(W_1)}{G_e(W_1 = 0)} = \frac{\beta(W_1)}{\beta(W_1 = 0)}$$

$$= 1 + \frac{D_{p2}\, L_{p1}}{D_{p1}\, W_2} \quad \text{for } W_1 > L_{p1}$$

In the above equation, subscript "1" refers to crystalline silicon, and subscript "2" refers to polysilicon over the crystalline silicon.

Using the dictates of the above theory, experiments have been initiated to fabricate solar cells using polysilicon in the emitter using low-resistivity float-zone wafers first to verify the process and designs, and subsequently transferring this to low-resistivity web silicon. Undoped polysilicon will be deposited by the low-pressure chemical vapor deposition (LPCVD) technique. The polysilicon will be doped by a $POCl_3$ diffusion, and the polygrid lines will be initially defined by ion milling or reactive ion etching. Two initial cell designs are shown schematically in Figure 1. It should be recognized that in order for the polysilicon emitter or grid to be really effective, one should have a cell where the base recombination has been minimized and the V_{oc} is limited by the emitter recombination or the recombination under the contact grid. Similarly, in a base-controlled cell, p^+-polysilicon deposition can be used instead of the conventional BSF to obtain a higher V_{oc}.

Preliminary results on this approach are presented in the next section.

3.2 Results On Cells With Polysilicon/Ti-Pd-Ag Grid

We have completed the first run with a polysilicon grid. After the boron BSF on the back side, 2800 Å poly were deposited on the front side by LPCVD at 625°C by thermal decomposition of silane (SiH_4). The $POCl_3$ diffusion was performed at 950°C instead of the conventional 850°C to allow enough phosphorus to diffuse through the poly and into the single-crystal region. Figure 1 shows a spreading resistance profile after the $POCl_3$ diffusion. The surface concentration was ~2 x $10^{20}cm^{-3}$ and the junction depth was ~0.45 μm. Notice that the profile is so smooth that it is difficult to tell where the silicon/polysilicon boundary is.

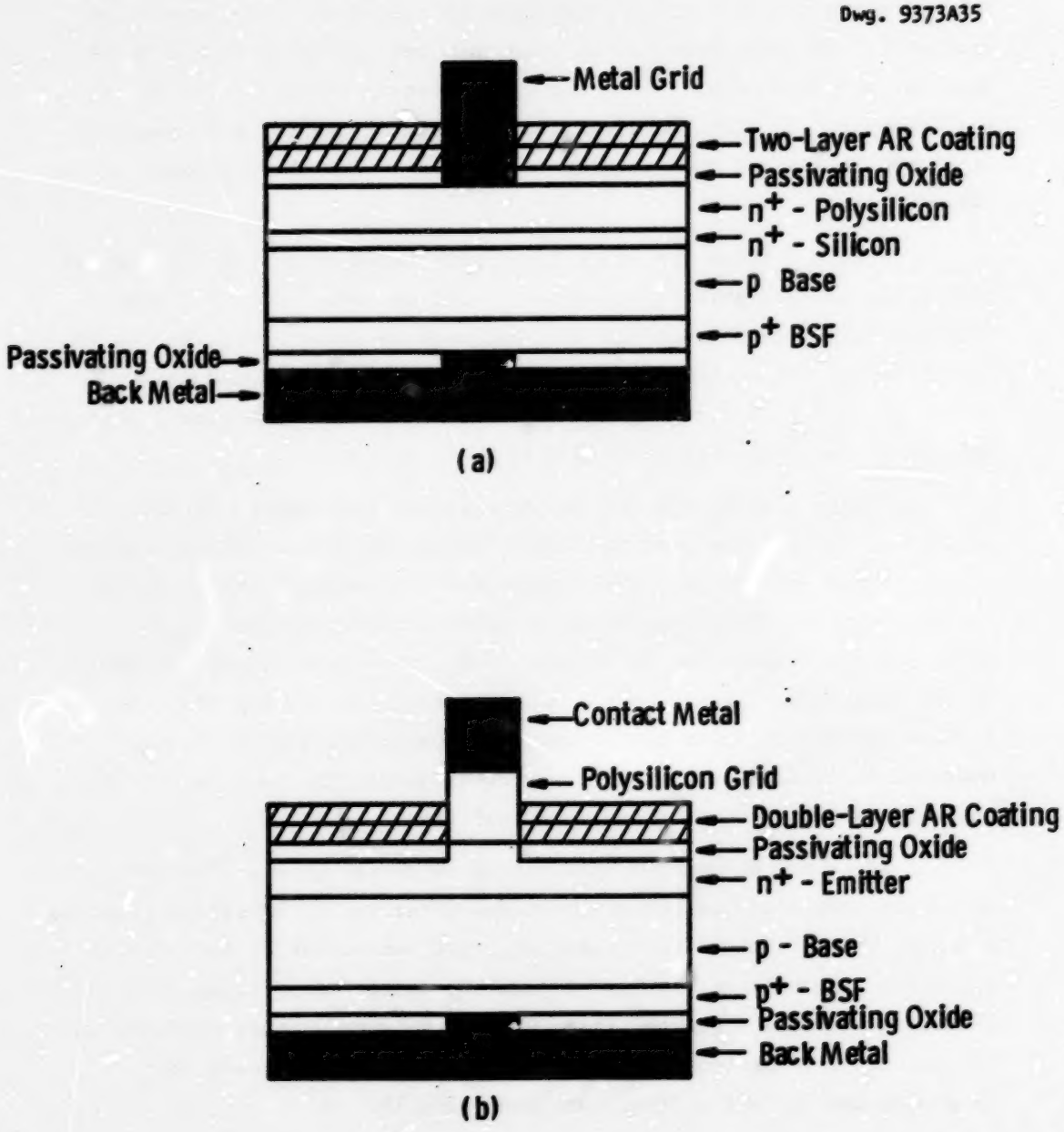

Figure 1. Polysilicon emitter/grid designs for high-efficiency solar cells

After the $POCl_3$ diffusion through the poly, the polysilicon was etched off by argon ion-milling at a rate of ~400 Å/min; a 6-3/4 to 7 min etching was just about sufficient to remove the poly layer. At this point the experiment was divided into two parts: a) in the first part the poly was removed from the entire wafer, and b) in the second part the polygrid lines were defined by covering the polygrid regions with photoresist and then etching the poly off from the remainder of the wafer.

Figure 3 shows the polysilicon grid lines after ion-milling; at this stage the polygrid lines are very well defined. Figure 2 shows that the diffusion through the poly followed by ion-milling results in an emitter with a shallow junction (N_j ~ 0.2 μm) and reduced heavy doping (N_s ~ 3 x 10^{19} as opposed to 2 x 10^{20} cm^{-3}), which should also be beneficial for high-efficiency cells.

Figure 4 shows the reflection electron diffraction (Rheed) pattern of the silicon surface after ion-milling. It is clear from the haze and ring pattern that the surface has been damaged and it is not single crystal. Therefore, prior to oxide passivation the samples were heat treated at 800°C for 15 minutes in N_2. Figure 4b shows the spot pattern and Kikuchi lines in the Rheed pattern, indicating that the surface damage, at least the structural damage, has been restored. However, it is not clear if any electrical damage has been done or if the surface will require a longer anneal time.

After the N_2 anneal, passivating oxide was grown. The SPV diffusion length was measured before and after the N_2 anneal/passivation process. Table 1 shows that there was some indication of decrease in diffusion length after the heat treatment. After ion-milling, the diffusion length was greater than 200 μm, the same as that obtained in the conventional process, but in some cases after subsequent heat treatment the diffusion length dropped below 180 μm.

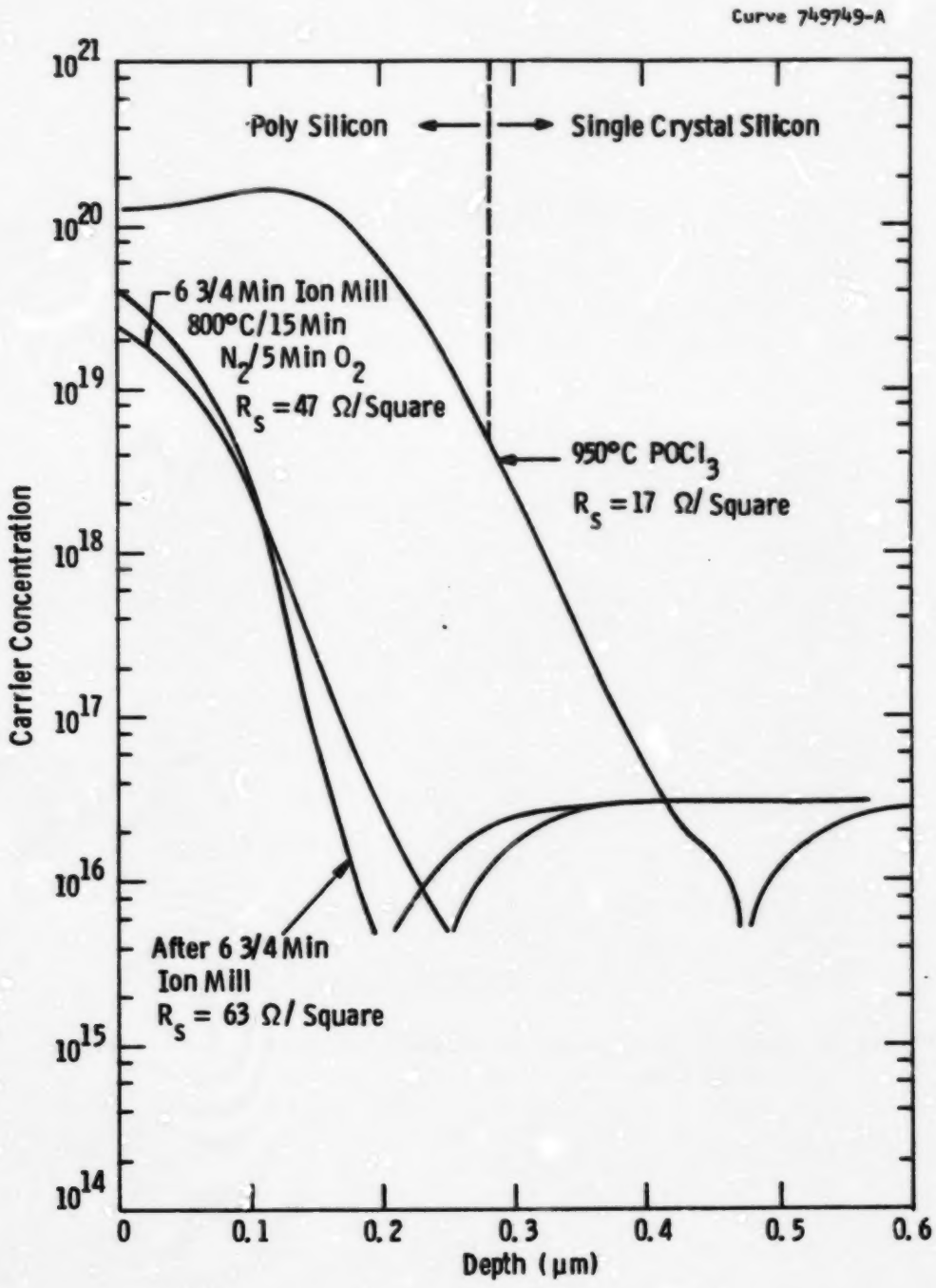

Figure 2. Spreading resistance profiles for: a) 2800 Å polysilicon deposition followed by 950°C $POCl_3$ diffusion; b) 6-3/4 ion milling after $POCl_3$ diffusion; c) ion milling followed by 800°C/15 minutes N_2/5 minute O_2 heat treatment

ORIGINAL PAGE IS
OF POOR QUALITY

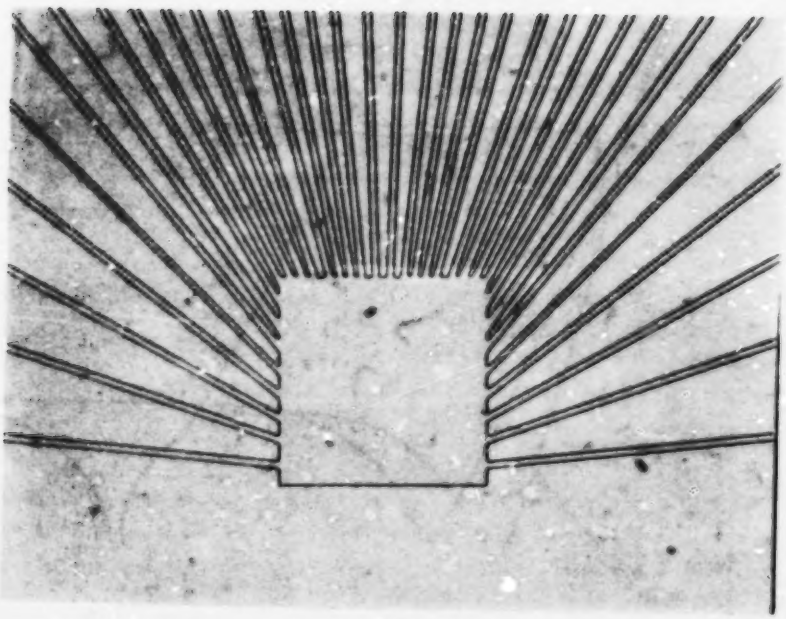

Figure 3. Optical photograph of polysilicon grid lines defined by ion milling

ORIGINAL PAGE IS
OF POOR QUALITY

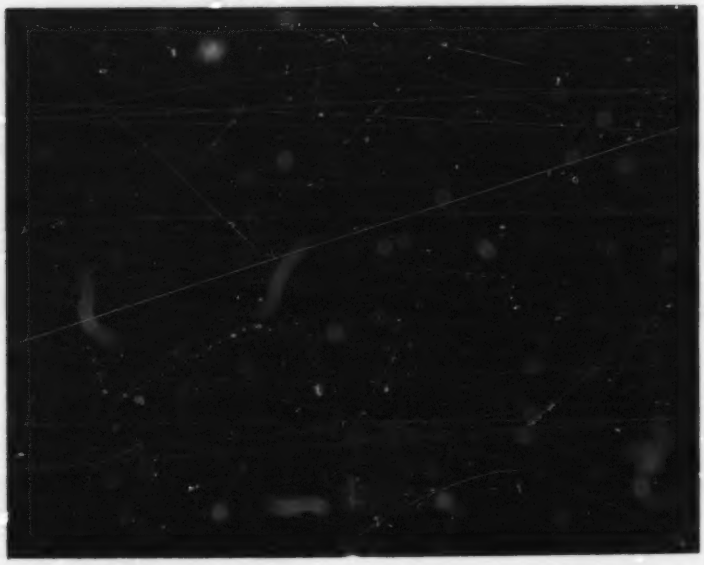

(a)

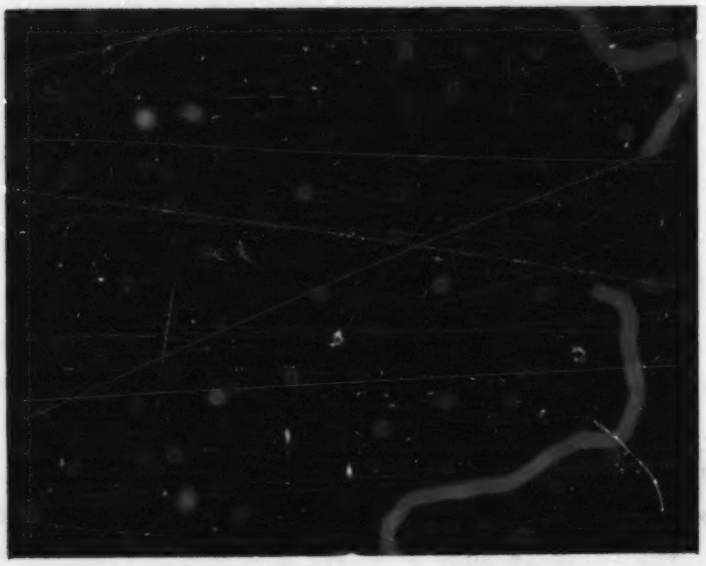

(b)

Figure 4. Reflection high-energy diffraction (Rheed) pattern of the: a) silicon surface after 6-3/4 minute argon ion milling, and b) ion-milled surface after 800°C/15 minute N_2/5 minute O_2 heat treatment

Table 1

SPV Diffusion Length Measurements After 6.75 min Ion Milling and Ion Milling Followed By 800°C/15 min N_2/5 min O_2 Heat Treatment

Sample Description		SPV Diffusion Length (μm)
Sample A:	After Ion Milling	260
	Ion Milling and Heat Treatment	174
Sample B:	After Ion Milling	189
	Ion Milling and Heat Treatment	190

After passivation, the oxide over the polygrid was removed and regular Ti-Pd-Ag metal was deposited over the polygrid lines by a combination of evaporation/rejection/Ag plating.

Thus, the above fabrication procedure resulted in all the cells having lower C_o (~2 x 10^{19} cm^{-3}) and some with or without the 0.28 μm thick polygrid lines underneath the Ti-Pd-Ag metal. Figure 1b shows the design with the polygrid.

Table 2 shows a comparison of the cell data for: a) conventional cells with no poly deposition and N_s = 2 x 10^{20} cm^{-3}, b) diffusion through polysilicon but no polygrid, and c) diffusion through polysilicon with the polygrid. These cells do not have any AR coating. The preliminary data in the table indicate that in this first solar cell run, cells with the polygrid show somewhat higher V_{oc} compared to the ones without the polygrid. However, cells with the polygrid are somewhat inferior to the conventional cells. Contrary to our expectation, V_{oc} did not increase; in both cases V_{oc} ~ 608 mV. The short-circuit current density in polygrid cells is 23.5 mA/cm^2, which is much less than in the conventional cells (25 mA/cm^2). This is primarily due to the lower lifetime in the polygrid cells (Table 1).

Thus, if the lifetime could have been retained in the polygrid cells, we might have seen a higher V_{oc}. This experiment will be repeated, along with some variation in the cell designs, such as leaving the polysilicon as part of the emitter (Figure 1a).

3.3 Resistivity and Lifetime Considerations For High-Efficiency Web Cells

The third quarterly report showed 16% efficient web solar cells on 4 ohm-cm web and 16.9% efficient web solar cells on 0.37 ohm-cm web crystal. The measured diffusion length (obtained by LCVD lifetime measurement) was ~ 250 μm in the 4 ohm-cm cell and 150 μm in the 0.37 ohm-cm cell. During this period model calculations were done to determine resistivity and diffusion length requirements for achieving 17-18% efficient web solar cells.

Needless to say, low-resistivity silicon with high minority carrier lifetime is an ideal candidate for high-efficiency solar cells. However, when the doping concentration exceeds $2 \times 10^{17} cm^{-3}$, Auger recombination begins to limit or lower the carrier lifetime ($\tau_A = \frac{1}{kN^2}$). Below this concentration, carrier lifetime is governed by a Kendall-like expression

$$\tau_k = \frac{\tau_o}{1 + \frac{N}{7 \times 10^{15}}}$$

which is also a function of doping concentration in the range of $10^{15} - 10^{17}\ cm^{-3}$.

We reported earlier that the diffusion length in as-grown dendritic web silicon is usually low (40 ± 20 μm) and it improves dramatically with high-temperature cell processing. The exact source of this phenomenon is not yet clear. However, it seems that quenched-in defects, stress, impurities, dislocations, and twin planes may be involved individually or collectively to give rise to this behavior. Thus, if the carrier lifetime in web silicon is primarily controlled by

Table 2

A Comparison of the Lighted I-V Data of:

a) Conventional Cell With No Poly/Deposition and $N_s = 2 \times 10^{20}$ cm^{-3}

b) Cell With Poly Deposition and Ion Milling and $N_s \sim 2 \times 10^{19}$ cm^{-3}

c) Poly Grid Cell with $N_s \sim 2 \times 10^{19}$ cm^{-3}

These Cells have No AR Coating.

Sample ID	Sample Description	V_{oc} mV	J_{sc} mA/cm^2	ff	η %
5-1	Conventional Cell	609	25.0	0.800	12.2
2-3	Poly Deposition and Ion Milling $N_s \sim 2 \times 10^{19}$ cm^{-3}	595	22.4	0.802	10.7
6-7	Poly Grid $N_s \sim 2 \times 10^{19}$ cm^{-3}	607	23.4	0.800	11.4

Run # HIEFY-23
AM1, 100 mW/cm^2 Illumination

the above defects (τ_d) and not by dopant concentration in the range of $10^{15} - 10^{17}$ cm^{-3} ($\frac{1}{\tau} = \frac{1}{\tau_A} + \frac{1}{\tau_b} + \frac{1}{\tau_d}$), then one would expect low-resistivity web silicon to give higher V_{oc} without much penalty in J_{sc} (some reduction in J_{sc} may come from reduced diffusivity or mobility at higher doping concentrations). However, if the defects only change τ_o, then the lifetime in web may still remain a function of N_A according to Kendall's expression. Therefore, we need to find the τ versus N_A relationship in web silicon in order to select the optimum resistivity.

The model calculations in Table 3 show that in order to achieve 17.5% efficient web cells, only a 125 μm diffusion length is required in 0.2 ohm-cm material; if using 4 ohm-cm web, a diffusion length of 467 μm is needed. Thus, low-resistivity silicon relaxes the diffusion length requirement for achieving the same cell efficiency. It should be

realized that the calculations in Table 3 are true only for 150 μm thick web cells with both front and back surfaces passivated ($S_{on}^{+} = S_{op}^{+} =$ 500 cm/sec); a 0.2 μm deep emitter with $N_s = 2 \times 10^{20}$ cm^{-3} and $N_{xj} = 3 \times 10^{17}$ cm^{-3}; and a combined loss of 10% efficiency due to reflection, shadowing, and resistances. These calculations do not include any losses that may occur due to twin plane activity in the web.

Table 3

Model Calculations For Resistivity and Diffusion Length Requirements For 17.5% Efficient Web Solar Cells

$W = 150$ μm
$S_{on}^{+} = 500$ cm/sec
$S_{op}^{+} = 500$ cm/sec
$S_{p-p}^{+} = 100$ cm/sec
$N_s = 2 \times 10^{20}$ cm^{-3}
$N_{xj} = 3 \times 10^{17}$ cm^{-3}

ρ ohm-cm	L μm	J_{sc} mA/cm^2	V_{oc} Volts	η %
4.0	360	35.0	.589	17.0
4.0	467	35.2	.597	17.5
0.2	360	35.0	.643	18.8
0.2	125	33.2	.634	17.5

We have recently started growing some low-resistivity web crystals and tracking their diffusion length in order to find out whether or not the diffusion length is a strong function of doping concentration in web.

In a few low-resistivity web crystals an as-grown diffusion length of 30 μm was measured, which went up to 150 μm after cell processing. According to model calculations, efficiencies greater than 17% could be achieved on this web crystal using advanced design features like oxide passivation, double-layer AR coating, and a back-surface reflector. A few 16.9% efficient cells were made on this web material, and more work is in progress.

4. PROGRAM STATUS

4.1 Present Status

The current milestone chart for this program is shown in Table 4. During this period we have:

- developed designs for polysilicon emitter solar cells,
- developed processes to fabricate polysilicon emitter/grid solar cells,
- fabricated solar cells with polysilicon grid under the metal, and
- performed model calculations for the resistivity and lifetime considerations for web.

4.2 Future Activity

In the follow-on program the investigation of the use of the polysilicon emitter, BSF, or grid for high-efficiency web solar cells will be continued. Cell designs and a process sequence will be developed for fabricating low-resistivity high-efficiency web cells.

Table 4

MILESTONE CHART

		1984								1985	
		A	M	J	J	A	S	O	N	D	J	F
Task 1.	Investigate Lifetime in Web	▲	———	———	———	———	———	———	———	———	———	▲
Task 2.	Develop Process Techniques	▲	———	———	———	———	———	———	———	———	———	△
Task 3.	Reduce Surface Recombination	▲	———	———	———	———	———	———	———	———	△	
Task 4.	Provide Samples to JPL						▲				▲	△
Task 5.	Fabricate Web Solar Cells							▲	———	———	———	△
Task 6.	Support Meetings	As Required by JPL										
Task 7.	Documentation	▲	▲	▲	▲	▲	▲	▲	▲	▲	▲	△

5. REFERENCES

1. T. H. Ning and R. D. Isaac, IEEE Trans. on Electron Devices, Vol ED-27, No. 11, p. 2051 (1980).

2. H. C. DeGraaff and J. Gerard DeGroot, IEEE Trans. on Electron Devices, Vol. ED-26, No. 11, p. 1771 (1979).

3. P. Ashburn and B. Soerowirdjo, IEEE Trans. on Electron Devices, Vol. ED-31, No. 7, p. 853 (1984).

4. W.J.M.J. Josquin, P. R. Boudewijn and Y. Tamminga, Appl. Phys. Let. Vol. 43, Noa. 10, p. 962 (1983).

5. P. Ashburn and B. Soerowirdjo, Solid-State Electronics, Vol 24, p. 475 (1981).

6. ACKNOWLEDGEMENTS

The authors would like to thank J. B. McNally, F. S. Youngk, and G. J. Machiko for cell fabrication; S. Karako for cell testing, surface photovoltage measurements, and assisting with the model calculations.